A Note on Reassigned Gabor Spectrograms of Hermite Functions

Patrick Flandrin

Journal of Fourier Analysis and Applications

ISSN 1069-5869

J Fourier Anal Appl
DOI 10.1007/s00041-012-9253-2

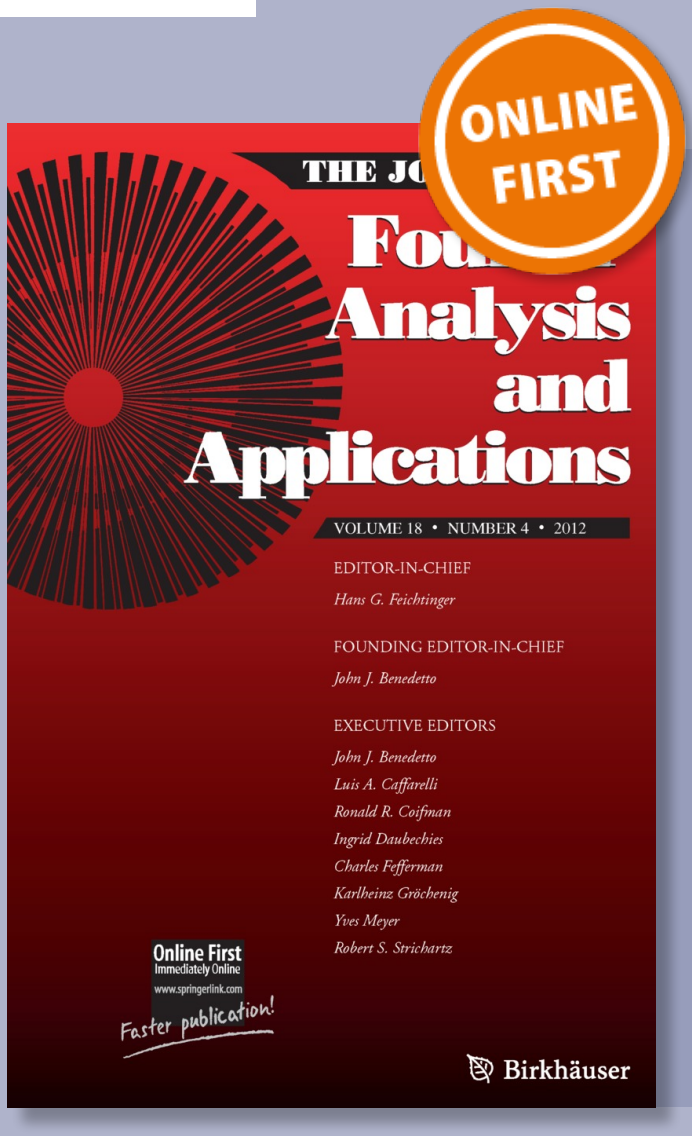

Springer

Your article is protected by copyright and all rights are held exclusively by Springer Science +Business Media New York. This e-offprint is for personal use only and shall not be self-archived in electronic repositories. If you wish to self-archive your work, please use the accepted author's version for posting to your own website or your institution's repository. You may further deposit the accepted author's version on a funder's repository at a funder's request, provided it is not made publicly available until 12 months after publication.

Author's personal copy

J Fourier Anal Appl
DOI 10.1007/s00041-012-9253-2

A Note on Reassigned Gabor Spectrograms of Hermite Functions

Patrick Flandrin

Received: 25 May 2012 / Revised: 12 June 2012
© Springer Science+Business Media New York 2012

Abstract An explicit form is given for the reassigned Gabor spectrogram of an Hermite function of arbitrary order. It is shown that the energy concentration sharply localizes outside the border of a clearance area limited by the "classical" circle where the Gabor spectrogram attains its maximum value, with a perfect localization that can only be achieved in the limit of infinite order.

Keywords Gabor transform · Hermite functions · Time-frequency analysis · Reassignment

Mathematics Subject Classification 42C40 · 42A38 · 94A12

1 Motivation

1.1 Why Hermite functions?

Hermite functions form a family of orthonormal functions that are important and useful in many respects. One can first mention that they are eigenfunctions of the Fourier transform [7], thus generalizing the well-known relationship which holds for the Gaussian function, the latter happening to be precisely the first Hermite function. As a consequence, Hermite functions are also naturally encountered in a variety of "uncertainty" questions constraining a function and its Fourier transform. They are in particular eigenfunctions of localization operators in the time-frequency plane, with respect to either elliptic indicator functions in the Wigner representation

Communicated by Hans G. Feichtinger.

P. Flandrin (✉)
École Normale Supérieure de Lyon, Laboratoire de Physique (UMR 5672 CNRS), 46 allée d'Italie, 69364 Lyon Cedex 07, France
e-mail: flandrin@ens-lyon.fr

Published online: 04 December 2012

Author's personal copy

[8, 9] or Gaussian-shaped weightings applied to Gabor transforms [6]. This makes them particularly useful in the context of multitaper time-frequency analysis [3, 16]. From a more physical perspective, Hermite functions are stationary eigenstates of the quantum harmonic oscillator [5], with phase-space diagrams that restrict to circles $p^2 + q^2 = C$ in the classical limit.

1.2 Why Reassigned Gabor Spectrograms?

This note is concerned with Hermite functions considered as functions of the time variable, and its purpose is to investigate their localization properties in the time-frequency plane. This will be done within the specific framework of Gabor spectrograms, because they are positive energy distributions with minimum spread [14]. This will involve furthermore a reassignment step [10, 15] so as to increase localization. It is known in fact [10] that reassignment allows for a perfect localization in the case of unimodular linear chirps defined as

$$c(t) = e^{i(\alpha t^2 + \beta t + \gamma)}; \quad (\alpha, \beta, \gamma \in \mathbb{R}), \tag{1}$$

and one of the questions to be answered in this note—suggested by observations reported, e.g., in [4], Chap. 1, Fig. 1.6—is to establish whether such a perfect localization is attained for Hermite functions too (it will be shown in Sect. 3.3 that this is true only in some asymptotical sense).

2 Hermite, Wigner and Gabor

We consider orthonormal Hermite functions defined as

$$h_k(t) = C_{k-1} \frac{1}{\sqrt{T}} H_{k-1}(\sqrt{2\pi}\, t/T) e^{-\pi (t/T)^2}, \tag{2}$$

where

$$H_n(\alpha) = (-1)^n e^{\alpha^2} \frac{d^n}{d\alpha^n} e^{-\alpha^2}, \quad n = 0, 1, \ldots \tag{3}$$

is the Hermite polynomial of degree n [1], $C_n = 1/\sqrt{2^{n-1/2} n!}$ and $T > 0$ is some time scaling parameter.

If we define the Wigner distribution of a square-integrable function $x(t) \in L^2(\mathbb{R})$ as

$$W_x(t, \omega) = \int_{-\infty}^{+\infty} x\left(t + \frac{1}{2}\tau\right) \overline{x\left(t - \frac{1}{2}\tau\right)} e^{-i\omega\tau}\, d\tau, \tag{4}$$

we know (see, e.g. [12] and references therein) that

$$W_{h_k}(t, \omega) = v_{k-1}\big((t/T)^2 + (T\omega/2\pi)^2\big), \tag{5}$$

where v_k involves the Laguerre polynomial of order k. In the general case of an arbitrary T, this expression exhibits an elliptic symmetry which reduces to a circular one (in the sense that (5) only depends on $t^2 + \omega^2$) for the specific choice $T = \sqrt{2\pi}$.

Author's personal copy

While most of the following results could be derived in the elliptic case, we will restrict to the circular case from now on.

Turning to Gabor spectrograms (i.e., squared magnitudes of those short-time Fourier transforms which are based on a Gaussian window, something which is also sometimes referred to as Husimi functions [13]), we will therefore make the explicit choice of the unit-energy Gaussian window

$$g(t) = \pi^{-\frac{1}{4}} e^{-\frac{1}{2}t^2}, \tag{6}$$

which is itself "circular" in the sense that its Wigner distribution reads

$$W_g(t,\omega) = 2\, e^{-(t^2+\omega^2)}. \tag{7}$$

Given this window, we know that the associated Gabor spectrogram

$$\begin{aligned} S_{h_k}^{(g)}(t,\omega) &= \left| \int_{-\infty}^{+\infty} h_k(s) g(s-t) e^{-i\omega s} ds \right|^2 \\ &= \frac{1}{\sqrt{\pi}} \left| \int_{-\infty}^{+\infty} h_k(s) e^{-\frac{1}{2}(s-t)^2} e^{-i\omega s} ds \right|^2 \end{aligned} \tag{8}$$

of $h_k(t)$ can be equivalently expressed as [9]

$$S_{h_k}^{(g)}(t,\omega) = \frac{1}{\pi} \iint_{-\infty}^{+\infty} W_{h_k}(s,\xi) e^{-[(s-t)^2+(\xi-\omega)^2]} ds\, d\xi, \tag{9}$$

and it readily follows from (5) and (7) that it enjoys a circular symmetry too. In order to evaluate explicitly this quantity, it is therefore sufficient to compute

$$V(t) = S_{h_k}^{(g)}(t,0) = \frac{1}{\sqrt{\pi}} \left| \int_{-\infty}^{+\infty} h_k(s) e^{-\frac{1}{2}(s-t)^2} ds \right|^2 \tag{10}$$

and to deduce from this section at $\omega = 0$ the whole desired spectrogram as

$$S_{h_k}^{(g)}(t,\omega) = V\left(\sqrt{t^2+\omega^2}\right). \tag{11}$$

Expressing $V(t)$ (in the circular case where $T = \sqrt{2\pi}$) as

$$V(t) = \frac{1}{\pi\sqrt{2\pi}} \left| C_{k-1} \int_{-\infty}^{+\infty} H_{k-1}(s) e^{-\frac{1}{2}s^2} e^{-\frac{1}{2}(s-t)^2} ds \right|^2, \tag{12}$$

reorganizing the terms in the exponential and making use of the identity ([11], Eq. 7.374.6)

$$\int_{-\infty}^{+\infty} H_n(x) e^{-(x-y)^2} dx = \sqrt{\pi}\, y^n 2^n, \tag{13}$$

we end up with

$$V(t) = \frac{1}{2^{k-1}(k-1)!} t^{2(k-1)} e^{-\frac{1}{2}t^2}. \tag{14}$$

It thus follows from (11) that we have

$$S_{h_k}^{(g)}(t,\omega) = \frac{1}{2^{k-1}(k-1)!} \left(t^2+\omega^2\right)^{k-1} e^{-\frac{1}{2}(t^2+\omega^2)} \tag{15}$$

Author's personal copy

and, therefore,

$$M_{h_k}^{(g)}(t,\omega) = \frac{1}{\sqrt{2^{k-1}(k-1)!}}\left(t^2+\omega^2\right)^{\frac{k-1}{2}} e^{-\frac{1}{4}(t^2+\omega^2)}, \tag{16}$$

with $M_{h_k}^{(g)}(t,\omega)$ the magnitude of the corresponding short-time Fourier (Gabor) transform.

3 Reassignment

3.1 Principle

The starting point of reassignment is to re-express a spectrogram, usually defined as the squared magnitude of a short-time Fourier transform, as the 2D smoothing of the Wigner distribution of the signal by that of the window:

$$S_x^{(h)}(t,\omega) = \iint_{-\infty}^{+\infty} W_x(s,\xi)\, W_h(s-t,\xi-\omega)\, \frac{ds d\xi}{2\pi}. \tag{17}$$

This general result [9]—that echoes the special case (9) of the Gabor spectrogram which makes use of a Gaussian window—allows for a simple interpretation: the value of a spectrogram at some given time-frequency point (t,ω) results from the summing up of all local values of the Wigner distribution within a time-frequency domain whose extension is controlled by the window. Unless such values would be symmetrically distributed around it, the geometrical center of this domain has however no reason to be chosen as the locus where to assign the integrated local energy. Indeed, a more meaningful location is the centroid $(\hat{t}(t,\omega), \hat{\omega}(t,\omega))$ of the Wigner distribution values within the domain, defined as

$$\hat{t}(t,\omega) = \frac{1}{S_x^{(h)}(t,\omega)} \iint_{-\infty}^{+\infty} s\, W_x(s,\xi)\, W_h(s-t,\xi-\omega)\, \frac{ds d\xi}{2\pi}; \tag{18}$$

$$\hat{\omega}(t,\omega) = \frac{1}{S_x^{(h)}(t,\omega)} \iint_{-\infty}^{+\infty} \xi\, W_x(s,\xi)\, W_h(s-t,\xi-\omega)\, \frac{ds d\xi}{2\pi}. \tag{19}$$

The purpose of reassignment is precisely to move each spectrogram value from the point (t,ω) where it has been computed to such a centroid:

$$S_x^{(h)}(t,\omega) \to \hat{S}_x^{(h)}(t,\omega) = \iint_{-\infty}^{+\infty} S_x^{(h)}(s,\xi)\, \delta\big(t-\hat{t}(s,\xi), \omega-\hat{\omega}(s,\xi)\big)\, \frac{ds d\xi}{2\pi}. \tag{20}$$

3.2 Explicit Form

In its original formulation [15], reassignment was computed from the phase information contained in the complex-valued short-time Fourier transform with window $h(t)$. It has then been shown (see [10] and references therein) that a more efficient identification of the centroids coordinates could be achieved by a suitable combination of two additional short-time Fourier transforms based on the companion windows $t.h(t)$

Author's personal copy

and $dh(t)/dt$ [10]. More recently [2], a third possibility has been proposed for Gabor spectrograms, which derives reassignment shifts from the magnitude of the Gabor transform. This reads

$$\hat{t}(t,\omega) = t + \frac{\partial}{\partial t}\log M_{h_k}^{(g)}(t,\omega); \tag{21}$$

$$\hat{\omega}(t,\omega) = \omega + \frac{\partial}{\partial \omega}\log M_{h_k}^{(g)}(t,\omega), \tag{22}$$

leading, in the present case (16), to

$$\hat{t}(t,\omega) = \frac{t}{2} + (k-1)\frac{t}{t^2+\omega^2}; \tag{23}$$

$$\hat{\omega}(t,\omega) = \frac{\omega}{2} + (k-1)\frac{\omega}{t^2+\omega^2}. \tag{24}$$

Based on (15), it is easy to check that the Gabor spectrogram attains its maximum value for coordinates (t_m, ω_m) such that

$$t_m^2 + \omega_m^2 = 2(k-1). \tag{25}$$

For $k = 1$, this reduces to a single point—namely the origin $(0, 0)$ of the plane—but, for $k > 1$, this corresponds to circles which happen to be fixed points of the reassignment operator. For any point on concentric circles of the form

$$t^2 + \omega^2 = 2\rho(k-1), \quad \rho > 0, \tag{26}$$

we get

$$\hat{t}^2 + \hat{\omega}^2 = \left(t_m^2 + \omega_m^2\right)\frac{(\rho+1)^2}{4\rho}, \tag{27}$$

evidencing the fact that reassigned values are themselves located on circles which are concentric to the "classical" one given by (25), but do not identify to it as long as $\rho \neq 1$. *Reassignment does not lead therefore to a perfect localization.*

It is worth noticing that the factor $K(\rho) = (\rho+1)^2/4\rho$ which appears in the above expression (27) is such that $K(1/\rho) = K(\rho)$, allowing to consider all spectrogram values to be reassigned by varying ρ from 1 to $+\infty$. It furthermore satisfies $K(\rho) \geq 1$, with $K(1) = 1$. This means that, for a given order k, the reassigned values all lie in the domain

$$\mathcal{D} = \left\{(t,\omega) \mid t^2 + \omega^2 \geq t_m^2 + \omega_m^2 = 2(k-1)\right\}, \tag{28}$$

i.e., outside a clearance area limited by the "classical" circle where the Gabor spectrogram attains its maximum value.

Going back to (24), we readily get

$$\frac{\hat{\omega}(t,\omega)}{\hat{t}(t,\omega)} = \frac{\omega}{t}, \tag{29}$$

justifying that reassignment is operated radially in the time-frequency plane. Using again the circular symmetry argument, reassigning the Gabor spectrogram amounts therefore to evaluate

Author's personal copy

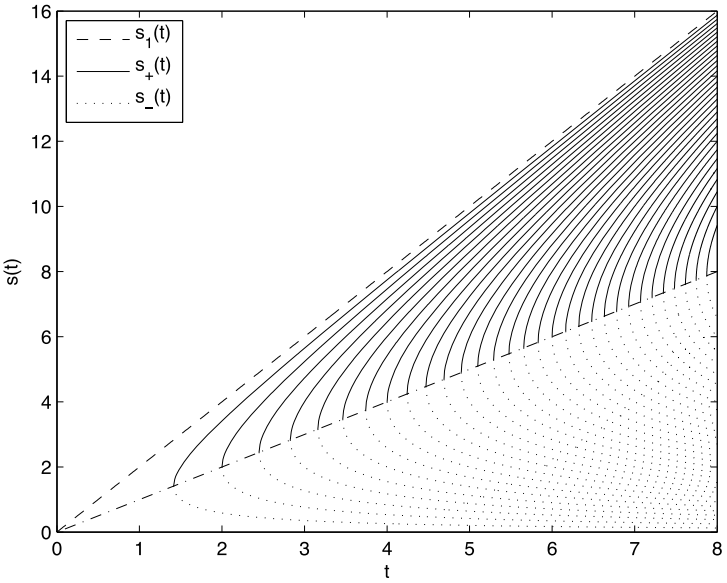

Fig. 1 Solutions (31) of the reassignment equations for positive times. The *dashed*, *full* and *dotted lines* correspond to the solutions referred to respectively as $s_1(t)$, $s_+(t)$ and $s_-(t)$ in the text, with the Hermite function order increasing from 1 to 33 when going from left to right. The locus of fixed points for the reassignment operators has been superimposed as the *dashed-dotted line*

$$\hat{S}_x^{(h)}(t,\omega) = \iint_{-\infty}^{+\infty} S_x^h(s,\xi)\delta\Big(\sqrt{t^2+\omega^2} - \hat{t}\Big(\sqrt{s^2+\xi^2}\Big)\Big)\frac{ds\,d\xi}{2\pi}$$
$$= \int_0^{+\infty} V(s)\,\delta\big(r-\hat{t}(s)\big)\,s\,ds =: \hat{V}(r), \tag{30}$$

with $r = \sqrt{t^2+\omega^2}$ and $V(t)$ as in (14).

In the present situation, the equation $\hat{t}(s) = t$ has one solution $s_1(t) = 2t$ when $k = 1$. When $k > 1$, it has two real-valued solutions $s_\pm(t)$, provided that $t^2 > 2(k-1)$. Considering only the case where $t \geq 0$, those solutions (which are displayed in Fig. 1) read

$$s_\pm(t) = t \pm \sqrt{t^2 - 2(k-1)}, \tag{31}$$

thus leading to

$$\hat{V}(r) = V\big(s_+(r)\big)\,s_+(r)\,J_+(r) + V\big(s_-(r)\big)\,s_-(r)\,J_-(r), \tag{32}$$

with

$$J_\pm(s) = \left|\frac{d\hat{t}}{ds}\big(s_\pm(s)\big)\right|^{-1} = \frac{s_\pm^2(s)}{|s_\pm^2(s) - 2(k-1)|}, \tag{33}$$

whence the final result

$$\hat{S}_{h_k}^{(g)}(t,\omega) = \frac{1}{2^{k-1}(k-1)!}\hat{V}\big(\sqrt{t^2+\omega^2}\big)\mathbf{1}_{\mathcal{D}}(t,\omega). \tag{34}$$

Author's personal copy

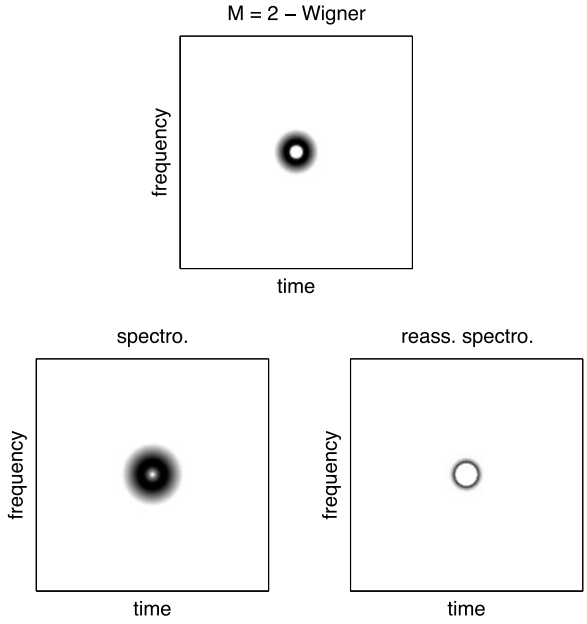

Fig. 2 Wigner distribution, spectrogram and reassigned Gabor spectrogram of Hermite function of order 2

It has to be remarked (cf. Fig. 1) that, except in the Gaussian case $k = 1$ for which the unique solution $s_1(t) = 2t$ is such that $(\partial s/\partial t)(0) = 2$, Eq. (31) has its two distinct solutions that both converge to the fixed point $t = \sqrt{2(k-1)}$ with an infinite slope. As a result, the summing up of the reassigned values accumulating on the border of the domain $\mathcal{D}$ diverges. This will be studied further in the next section.

3.3 Asymptotics

The limit behaviour of the expression (34) when $k > 1$ can be evaluated in two ways. Given a fixed order, we can first characterize more precisely the divergence of the reassigned spectrogram in the vicinity of the critical circle $t^2+\omega^2 = 2(k-1)$. Writing $t = \sqrt{2(k-1)} + \theta$, we get

$$\hat{V}(t) \sim \frac{[2(k-1)]^{k+\frac{1}{2}}}{\sqrt{\theta}} e^{-(k-1)} e^{-2\sqrt{k-1}\sqrt{\theta}}, \quad \theta \to 0_+. \tag{35}$$

Combining this approximation with (34) and considering in a second step that $k \to +\infty$, Stirling's formula allows for some further simplification that ends up with

$$\frac{1}{2^{k-1}(k-1)!} \hat{V}(t) \sim \frac{\sqrt{k-1}}{\sqrt{\theta}} e^{-2\sqrt{k-1}\sqrt{\theta}}, \quad k \to +\infty. \tag{36}$$

We see therefore that, for Hermite functions of growing order k, the width of the decaying exponential involved in (36) goes to zero as k is increased while its amplitude diverges to infinity, but in such a way that the overall integral of the right-hand side of (36) is unity. This justifies that, asymptotically,

$$\hat{S}_{h_k}^{(g)}(t,\omega) \overset{k\to\infty}{\longrightarrow} \delta\big(t^2+\omega^2-2(k-1)\big). \tag{37}$$

Author's personal copy

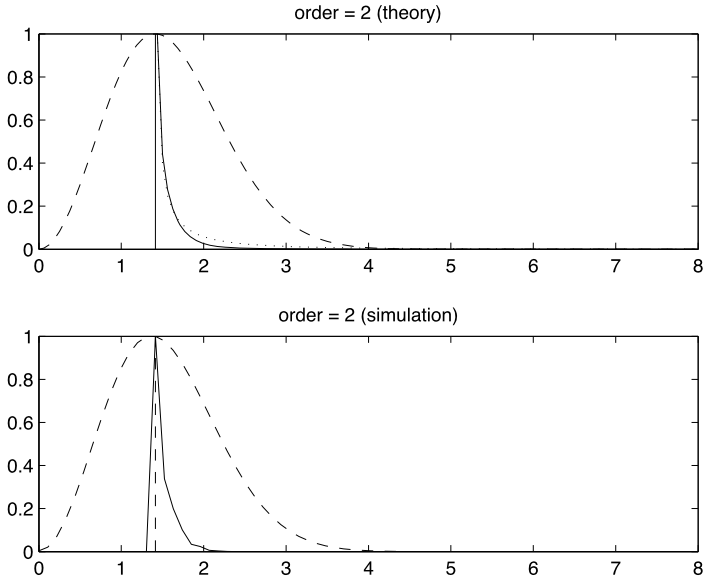

Fig. 3 Radial half-sections of the Gabor spectrogram (*dashed line*) and reassigned Gabor spectrogram (*full line*) of Hermite function of order 2. *Top*: theory (with approximation (36) in *dotted line*); *bottom*: from Fig. 2

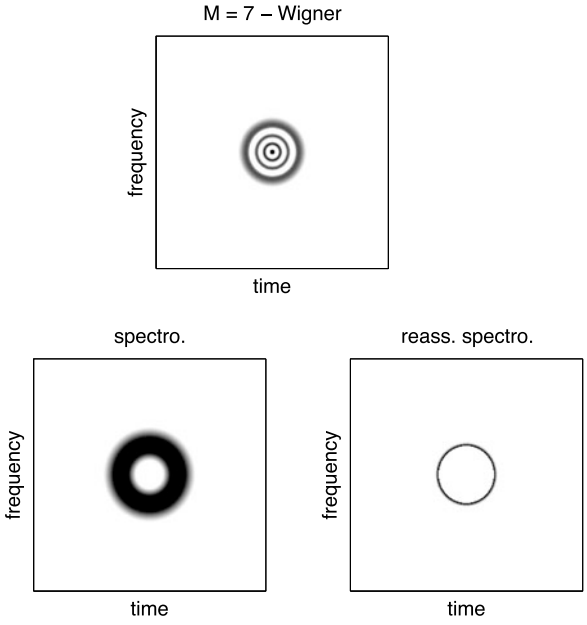

Fig. 4 Wigner distribution, spectrogram and reassigned Gabor spectrogram of Hermite function of order 7

This asymptotic regime, where $k \gg 1$, corresponds to a sharper and sharper energy localization on circles whose area $\mathcal{A}(k) = 2\pi(k-1)$ becomes larger and larger as compared to the minimum (Heisenberg) area $\mathcal{A}(1) = 2$, in accordance with the interpretation of such circles as "classical" trajectories in phase-space.

Author's personal copy

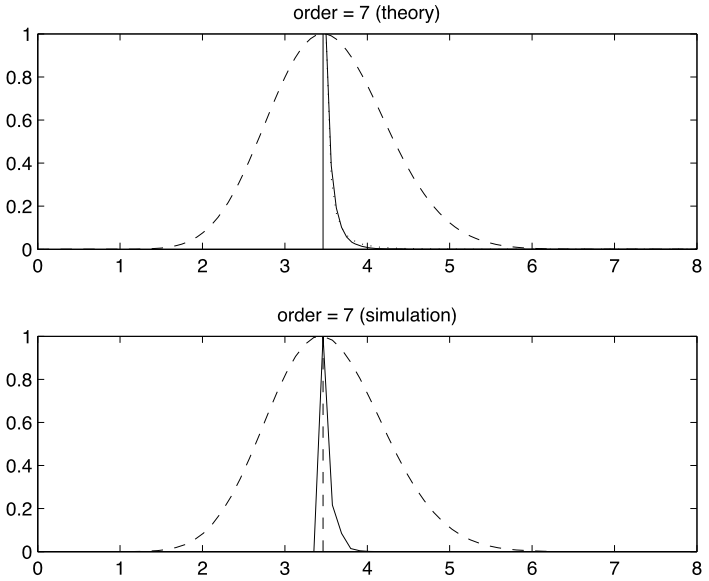

Fig. 5 Radial half-sections of the Gabor spectrogram (*dashed line*) and reassigned Gabor spectrogram (*full line*) of Hermite function of order 7. *Top*: theory (with approximation (36) in *dotted line*); *bottom*: from Fig. 4

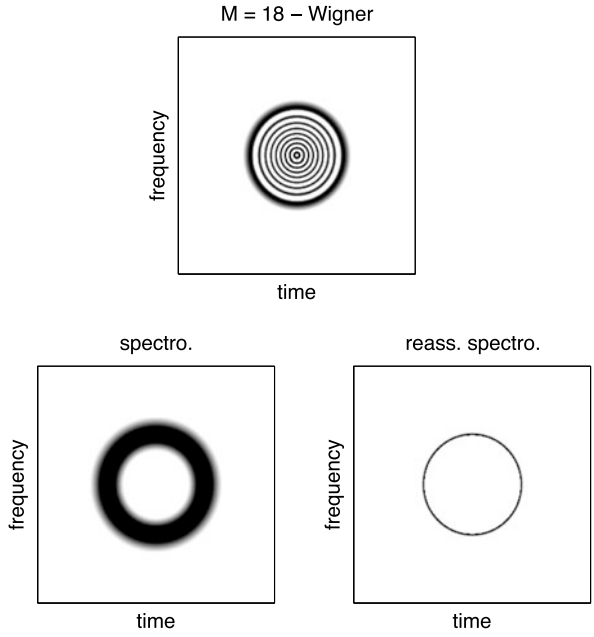

Fig. 6 Wigner distribution, spectrogram and reassigned Gabor spectrogram of Hermite function of order 18

3.4 Examples

Three examples supporting those computations are given in Figs. 2 to 7 (all time-frequency distributions are computed on a 256×256 grid).

Author's personal copy

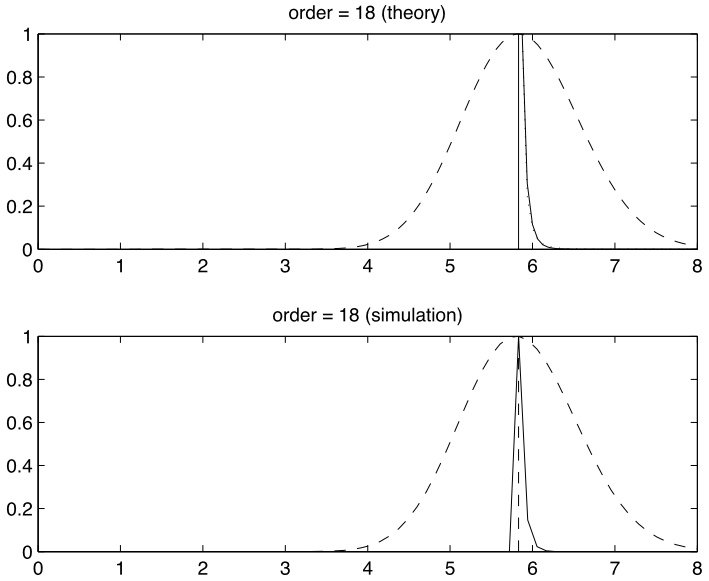

Fig. 7 Radial half-sections of the Gabor spectrogram (*dashed line*) and reassigned Gabor spectrogram (*full line*) of Hermite function of order 18. *Top*: theory (with approximation (36) in *dotted line*); *bottom*: from Fig. 6

4 Concluding Remarks

This note has made precise the way reassigned Gabor spectrograms localize the energy of Hermite functions in the time-frequency plane. It has been shown that a sharp localization is achieved on circles, tending to be perfect in the limit of infinite order. This asymptotic result can be viewed as a complement to the one stating that unimodular linear chirps have perfectly localized reassigned spectrograms. This however leaves open the question of whether those two types of waveforms are the only ones to guarantee such a perfect (asymptotic) localization.

References

1. Abramowitz, M., Stegun, I.: Handbook of Mathematical Functions. Dover, New York (1965)
2. Auger, F., Chassande-Mottin, E., Flandrin, P.: On phase-magnitude relationships in the short-time Fourier transform. IEEE Signal Process. Lett. **19**(5), 267–270 (2012)
3. Bayram, M., Baraniuk, R.G.: Multiple window time-varying spectrum estimation. In: Fitzgerald, W.J., et al. (eds.) Nonlinear and Nonstationary Signal Processing, pp. 292–316. Cambridge Univ. Press, Cambridge (2000)
4. Chassande-Mottin, E.: Méthodes de réallocation dans le plan temps-fréquence pour l'analyse et le traitement de signaux non stationnaires. Thèse de Doctorat. Université de Cergy-Pontoise (1998). Available on-line at http://www.apc.univ-paris7.fr/~ecm/98these/these/ecm98.html
5. Cohen-Tannoudji, C., Diu, B., Laloë, F.: Quantum Mechanics. Wiley, New York (1977)
6. Daubechies, I.: Time-frequency localization operators: a geometric phase-space approach. IEEE Trans. Inf. Theory **34**, 605–612 (1988)
7. Dym, H., McKean, H.P.: Fourier Series and Integrals. Academic Press, San Diego (1972)

Author's personal copy

8. Flandrin, P.: Maximum signal energy concentration in a time-frequency domain. In: Proc. of the IEEE Int. Conf. on Acoust., Speech and Signal Proc. ICASSP-88, New York, pp. 2176–2179 (1988)
9. Flandrin, P.: Time-Frequency/Time-Scale Analysis. Academic Press, San Diego (1999)
10. Flandrin, P., Auger, F., Chassande-Mottin, E.: Time-frequency reassignment—from principles to algorithms. In: Papandreou-Suppappola, A. (ed.) Applications in Time-Frequency Signal Processing, pp. 179–203. CRC Press, Boca Raton (2003). Chap. 5
11. Gradshteyn, I.S., Ryzikh, I.H.: Tables of Integrals, Series and Products, 5th edn. Academic Press, San Diego (1994)
12. Hlawatsch, F.: Time-Frequency Analysis and Synthesis of Linear Spaces. Kluwer Academic, Dordrecht (1998)
13. Husimi, K.: Some formal properties of the density matrix. Proc. Phys. Math. Soc. Jpn. **22**, 264–314 (1940)
14. Janssen, A.J.E.M.: Optimality property of the Gaussian window spectrogram. IEEE Trans. Signal Process. **39**, 202–204 (1991)
15. Kodera, K., Gendrin, R., de Villedary, C.: Analysis of time-varying signals with small BT values. IEEE Trans. Acoust. Speech Signal Process. **ASSP-26**(1), 64–76 (1978)
16. Xiao, J., Flandrin, P.: Multitaper time-frequency reassignment for nonstationary spectrum estimation and chirp enhancement. IEEE Trans. Signal Process. **55**(6 (Part 2)), 2851–2860 (2007)